

## New Liquid Crystal-Embedded PVdF-*co*-HFP-Based Polymer Electrolytes for Dye-Sensitized Solar Cell Applications

G. Vijayakumar, Meyoung Jin Lee, Myungkwan Song, and Sung-Ho Jin\*

Department of Chemistry Education, Interdisciplinary Program of Advanced Information and Display Materials,  
and Center for Plastic Information System, Pusan National University, Busan 609-735, Korea

Jae Wook Lee\*

Department of Chemistry, Dong-A University, Busan 604-714, Korea

Chan Woo Lee

Department of Chemistry, University of Ulsan, Ulsan 680-749, Korea

Yeong-Soon Gal

Polymer Chemistry Lab, Kyungil University, Hayang 712-70, Korea

Hyo Jin Shim and Yongku Kang

Advanced Materials Division, Korea Research Institute of Chemical Technology, Daejeon 305-600, Korea

Gi-Won Lee, Kyungkon Kim, and Nam-Gyu Park

Center for Energy Materials Research, Materials Science and Technology Division,  
Korea Institute of Science and Technology, Seoul 136-791, Korea

Suhkmann Kim\*

Department of Chemistry and Chemistry Institute for Functional Materials, Pusan National University, Busan 609-735, Korea

Received March 18, 2009; Revised June 26, 2009; Accepted June 30, 2009

**Abstract:** Liquid crystal (LC; E7 and/or ML-0249)-embedded, poly(vinylidenefluoride-*co*-hexafluoropropylene) (PVdF-*co*-HFP)-based, polymer electrolytes were prepared for use in dye-sensitized solar cells (DSSCs). The electrolytes contained 1-methyl-3-propylimidazolium iodide (PMII), tetrabutylammonium iodide (TBAI), and iodine ( $I_2$ ), which participate in the  $I_3^-/I^-$  redox couple. The incorporation of photochemically stable PVdF-*co*-HFP in the DSSCs created a stable polymer electrolyte that resisted leakage and volatilization. DSSCs, with liquid crystal (LC)-embedded PVdF-*co*-HFP-based polymer electrolytes between the amphiphilic ruthenium dye N719 absorbed to the nanocrystalline  $TiO_2$  photoanode and the Pt counter electrode, were fabricated. These DSSCs displayed enhanced redox couple reduction and reduced charge recombination in comparison to that fabricated from the conventional PVdF-*co*-HFP-based polymer electrolyte. The behavior of the polymer electrolyte was improved by the addition of optimized amounts of plasticizers, such as ethylene carbonate (EC) and propylene carbonate (PC). The significantly increased short-circuit current density ( $J_{sc}$ , 14.60 mA/cm<sup>2</sup>) and open-circuit voltage ( $V_{oc}$ , 0.68 V) of these DSSCs led to a high power conversion efficiency (PCE) of 6.42% and a fill factor of 0.65 under a standard light intensity of 100 mW/cm<sup>2</sup> irradiation of AM 1.5 sunlight. A DSSC fabricated by using E7-embedded PVdF-*co*-HFP-based polymer electrolyte exhibited a maximum incident photon-to-current conversion efficiency (IPCE) of 50%.

**Keywords:** liquid crystal, PVdF-*co*-HFP, polymer electrolyte, dye-sensitized solar cells, photovoltaic performance.

---

\*Corresponding Authors. E-mails: shjin@pusan.ac.kr  
or jlee@donga.ac.kr or suhkmann@pusan.ac.kr

## Introduction

Dye-sensitized solar cells (DSSCs) have received great interest in the context of renewable energy systems that rely on the conversion sun light to electric energy. In pioneering investigations, Grätzel and O'Regan developed simple and cost effective methods to fabricate DSSCs that are superior to those used to generate conventional Si-based solar cells.<sup>1-3</sup> A typical DSSC is comprised of four components, including (1) an electrode that consists of a fluorine-doped SnO<sub>2</sub> transparent conducting oxide (FTO) substrate, (2) a nanocrystalline TiO<sub>2</sub> layer containing a visible light absorbing dye, (3) a counter electrode consisting of Pt thin layer coated on top of a FTO substrate, and (4) a liquid electrolyte between the two electrodes that contains the redox couple ( $I_3^-/I^-$ ). High power conversion efficiencies (PCE, under 100 mW/cm<sup>2</sup> irradiation) reaching 11.18% have been obtained with DSSCs of this type. Unfortunately, the typical electrolytes used in these systems have several disadvantages including solvent leakage and evaporation, sealing difficulties, and electrode corrosion.<sup>4-6</sup>

Numerous efforts have been undertaken to develop DSSCs that do not contain liquid electrolytes. Several studies have explored gel or polymer electrolytes, such as organic and inorganic *p*-type semiconductors,<sup>7,8</sup> hole conductors,<sup>9-11</sup> and polymer and/or gel<sup>12-22</sup> materials, all incorporating ( $I_3^-/I^-$ ) as the redox couple. Among these approaches, those based on poly(vinylidenefluoride-*co*-hexafluoropropylene) (PVdF-*co*-HFP) have attracted the greatest interest owing to the photochemical stability of this material even in the presence of TiO<sub>2</sub> and Pt nanoparticles.<sup>23</sup> PVdF-*co*-HFP, combined with a room temperature ionic liquid (RTIL) as the iodide source (eg., 1-methyl-3-propylimidazolium iodide (PMII))<sup>24,25</sup> and a mixture of 1,2-dimethyl-3-propylimidazolium iodide (DMPII) and *N*-methylbenzimidazole (NMBI)),<sup>26</sup> comprise a family of polymer electrolytes that have been used in combination with the Z907 dye to fabricate DSSCs which have enhanced ionic conductivities and PCEs. RTILs serve as iodide sources as well as solvents in these electrolytes. DSSCs constructed following this design have several advantages that include low volatility, thermal stability, and nonflammability.<sup>27-29</sup> Moreover, a few studies have shown that the introduction of liquid crystals (LCs) in the polymeric electrolyte leads to an improvement of  $J_{sc}$  and the iodide exchange reaction, thus, an increase in chain mobility and the ionic conductivity.<sup>30-32</sup>

In recent investigations, we have explored the use of LC-embedded, PVdF-*co*-HFP-based, polymer electrolytes to enhance the ionic conductivity of polymer electrolytes and the photovoltaic performance of DSSCs made from these electrolytes. In the current effort, the photovoltaic performances, conductivities, and incident photon-to-current conversion efficiencies (IPCEs) of DSSCs, assembled with these electrolyte materials, have been elucidated. To the best of our knowledge, no prior work, aimed at development of

LC-embedded PVdF-*co*-HFP-based polymer electrolytes, has been performed.

## Experimental

**Materials.** PVdF-*co*-HFP ( $M_w$ : 400,000), I<sub>2</sub>, PC, and acetonitrile were obtained from Aldrich and used without further purification. PMII, TBAI, and EC were purchased from TCI Chemicals and used as received. Liquid crystal, E7 was purchased from Merck. N719 dye ([ $(C_4H_9)_4N$ ]<sub>2</sub> [Ru (II)L2-(NCS)2]), (where L=2, 2'-bipyridyl-4,4'-dicarboxylic acid, ruthenium TBA 535, Solaronix SA), nanocrystalline Ti-nanoxide HT/SP and platinum (Pt-catalyst T/SP) paste were purchased from Solaronix. FTO conductive glass substrates with a sheet resistance of 8 Ω/cm<sup>2</sup> were purchased from Hartford Glass, USA, and were used as substrates for the photoanode and counter electrode. The FTO plates were cut into 2 cm × 2 cm plates before use.

**Preparation of Electrolytes.** Four different electrolyte solutions were probed (Figure 1). The optimized PVdF-*co*-HFP-based polymer electrolyte consists of PVdF-*co*-HFP (0.132 g), TBAI (0.48 M), PMII (0.79 M), I<sub>2</sub> (0.23 M), EC (6.8 M), and PC (1.9 M) in acetonitrile (1 mL). To ensure homogeneity, the mixture was stirred continuously at 80 °C for 24 h. After cooling to room temperature, the stable viscous PVdF-*co*-HFP-based polymer electrolyte was used as a redox electrolyte for DSSCs. LC-embedded PVdF-*co*-HFP-based polymer electrolytes, having the composition described above, with equal amounts of PVdF-*co*-HFP and the LCs (E7 and/or ML-0249) were separately prepared. The liquid electrolyte was comprised of PMII (0.7 M), I<sub>2</sub> (0.03 M), GuSCN (0.05 M), TBP (0.5 M) in acetonitrile and valeronitrile (85:15 v/v) for comparison photovoltaic performances.

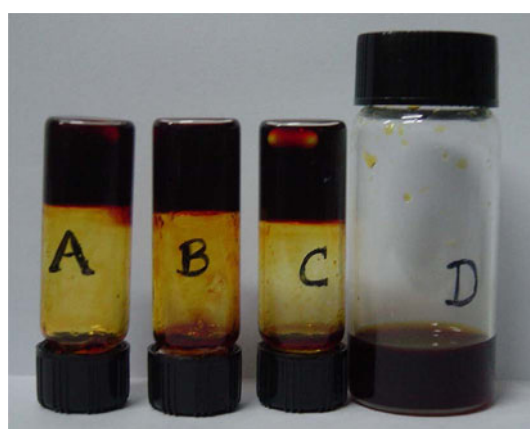


**Figure 1.** Photographs of electrolyte samples from left to right (a) conventional PVdF-*co*-HFP-based polymer electrolyte (the vial is upside down); (b) ML-0249:PVdF-*co*-HFP-based polymer electrolyte (the vial is upside down); (c) E7:PVdF-*co*-HFP-based polymer electrolyte (the vial is upside down); (d) liquid electrolyte.

### Preparation of the Photoanode and Counter Electrode.

A FTO glass substrate was washed thoroughly by using a sonicator and then coated with nanocrystalline TiO<sub>2</sub> paste (TiO<sub>2</sub>-nanoxide HT/SP, Solarnix) by using the doctor blade method. The thickness of the film was adjusted by using adhesive tape. After sintering the film at 480 °C for 0.5 h in air the coated FTO glass plate was cooled from 100 °C to 60 °C at a rate of 3 °C/min to avoid cracking of the 8 μm thick photoanode. The morphology of the photoanode was examined by using FE-SEM. In order to add the photosensitizer to the photoanode, the plate was immersed in a 0.5 mM solution of N719 dye in anhydrous ethanol overnight at room temperature. The TiO<sub>2</sub> photoanode (active area of 0.25 cm<sup>2</sup>) was then obtained by rinsing with anhydrous ethanol and drying with. The Pt counter electrode, which acts as a catalyst for the redox reaction on the coated FTO glass substrate, was prepared by using the doctor blade technique, described earlier.<sup>17</sup>

**Fabrication of and Measurement on DSSCs.** The PVdF-*co*-HFP-based polymer electrolytes were injected separately between the N719 dye adsorbed nanocrystalline TiO<sub>2</sub> photoanode through holes in the Pt counter electrode using a vacuum pump. After adding the hot electrolyte solution, the holes were sealed with a Surlyn sheet followed by a thin glass cover by heating. DSSC performances was determined by using a calibrated AM 1.5G solar simulator (Orel 300 W simulator, models 81150) with a light intensity of 100 mW/cm<sup>2</sup> adjusted using a standard PV reference cell (2 cm × 2 cm nanocrystalline silicon solar cell, calibrated at NREL, Colorado, USA) and a computer-controlled Keithley 236 source measure unit. The power conversion efficiency (PCE,  $\eta$ ) of a DSSC is given by

$$\eta = P_{out}/P_{in} = (J_{sc} \times V_{oc}) \times FF/P_{in} \quad (1)$$

with

$$FF = P_{max}/(J_{sc} \times V_{oc}) = (J_{max} \times V_{max})/(J_{sc} \times V_{oc}) \quad (2)$$

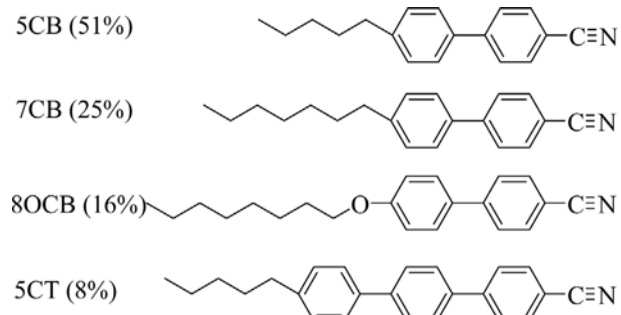
where  $P_{out}$  is the output electrical power of the device under illumination and  $P_{in}$  is the intensity of incident light (e.g., in W/m<sup>2</sup> or mW/cm<sup>2</sup>).  $V_{oc}$  is the open-circuit voltage,  $J_{sc}$  is the short-circuit current density, and fill factor (FF) is calculated from the values of  $V_{oc}$ ,  $J_{sc}$ , and the maximum power point,  $P_{max}$ . All fabrication steps and measurements were carried out in an ambient environment without a protective atmosphere. Conductivity measurements were performed by injecting electrolyte in between two ITO glass plates with Cu wire connection using Zahner Elektrik Model electrochemical impedance analyzer over a frequency range of 100 mHz to 1 MHz at various temperatures in the range of 25–80 °C with an AC amplitude of 10 mV. Each photovoltaic performance value is obtained by making at least three measurements. IPCE spectra were measured using a 300 W Xe lamp light source with monochromatic light in the range of 380–750 nm.

### Results and Discussion

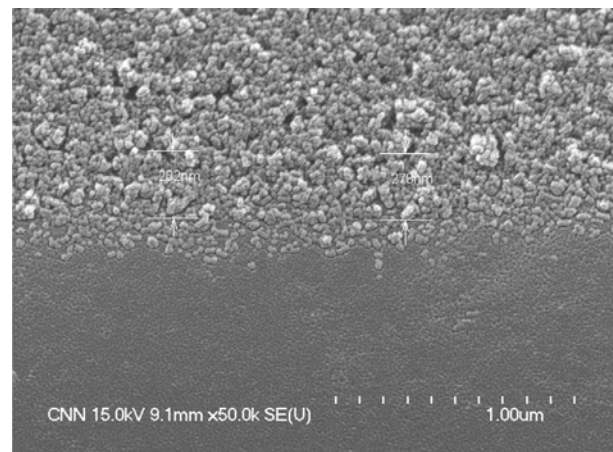
The liquid crystal E7, widely used in polymer dispersed liquid crystalline (PDLC) displays, was prepared by using the four CN-biphenyls shown in Figure 2. Another liquid crystal mixture probed in this study is ML-0249, which is often used for TFT-LCDs owing to its advantageous fast response time and low driving voltage.

In Figure 3 is shown a cross section image of 480 °C sintered, spherically shaped nanocrystalline TiO<sub>2</sub> (10 nm particle size) on a glass substrate. Numerous small pores exist on the photoanode, whose rough surface leads to enhanced adsorption of dyes that serve as photosensitizers. This results in improved light adsorption and an enhanced photovoltaic performance.

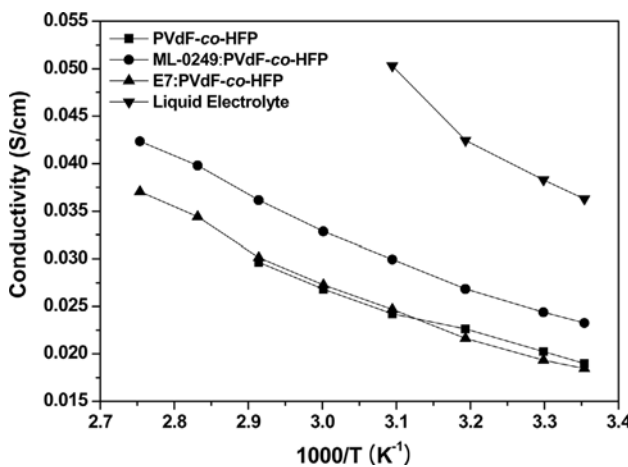
The temperature dependence of ionic conductivities of PVdF-*co*-HFP, ML-0249:PVdF-*co*-HFP, E7:PVdF-*co*-HFP, and a non-polymeric liquid electrolyte, are shown in the Figure 4. In all cases, ionic conductivity increases with increasing temperature. As the temperature increases, the free volumes of the electrolytes increase, resulting in an increase in the mobilities of ions on the LC-embedded PVdF-*co*-HFP-based polymer electrolyte matrix. The ionic conductivity of the conventional PVdF-*co*-HFP-based polymer electrolyte



**Figure 2.** Molecular structures and composition of E7 liquid crystal.



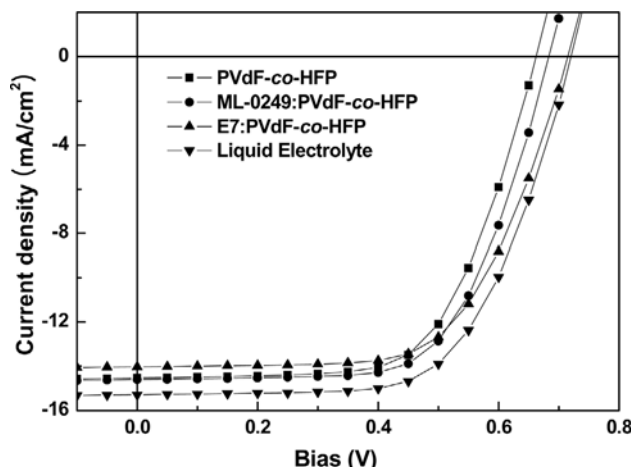
**Figure 3.** FE-SEM cross section images of the TiO<sub>2</sub> photoanode.

**Figure 4.** Ionic conductivity of electrolytes.

at 25 °C is *ca.*  $1.90 \times 10^{-2}$  S/cm (Table I). However, ML-0249- and E7-embedded PVdF-*co*-HFP polymer electrolytes display larger conductivities of  $2.33 \times 10^{-2}$  S/cm and  $1.85 \times 10^{-2}$  S/cm, respectively. These values are an order of magnitude larger than those previously reported.<sup>23</sup> This phenomenon is likely a consequence of enhanced ionic charge transfer in the redox couple ( $I_3^-/I$ ) and an increase in the miscibility of the electrolyte. The interaction of ML-0249 and  $I_2$  on the PVdF-*co*-HFP matrix provides a favorable conduction pathway leading to an enhancement of the  $I_3^-/I$  ionic mobility.

Owing to the presence of cyano groups in E7, its addition to the PVdF-*co*-HFP-based polymer electrolyte causes only a small change. This be the result of variations of charge carriers and the viscosity of the electrolyte. The presence of LCs in PVdF-*co*-HFP-based polymer electrolytes creates an additional conductive pathway, which holds the iodide sources and organic plasticizers on the polymer matrix during conduction. Ions in the redox couple ( $I_3^-/I$ ) migrate using at least two routes, involving movement through (1) pathways provided by the polymer with plasticizer present in the electrolyte, and (2) tunnels provided by the LC molecular chain. In contrast to liquid and conventional PVdF-*co*-HFP-based polymer electrolytes, the LC embedded PVdF-*co*-HFP-based polymer electrolytes display linear temperature dependent enhancements in conductivity and a thermal stabilities.

Current density-voltage (*J-V*) curves, measured under AM

**Figure 5.** J-V curves for DSSCs.

1.5G, for DSSCs, prepared by using the conventional PVdF-*co*-HFP-based polymer electrolyte, the LC-embedded PVdF-*co*-HFP polymer electrolytes, and a liquid electrolyte, are shown in Figure 5. The corresponding photovoltaic parameters of the DSSCs are listed in Table I. The respective  $J_{sc}$ ,  $V_{oc}$ ,  $FF$ , and PCE are 14.53 mA/cm<sup>2</sup>, 0.66 V, 0.63, and 6.07% for the DSSC made from the conventional PVdF-*co*-HFP-based polymer electrolyte. In contrast, the DSSC with an ML-0249-embedded PVdF-*co*-HFP-polymer electrolyte displays larger  $J_{sc}$  (14.60 mA/cm<sup>2</sup>) and  $V_{oc}$  (0.68 V) values that result in a PCE of 6.42%. The *ca.* 20 mV larger  $V_{oc}$  associated with the DSSC containing the ML-0249-embedded polymer electrolyte can be attributed to the difference between the Fermi level for electrons in the nanocrystalline TiO<sub>2</sub> electrode and the potential of redox couple ( $I_3^-/I$ ). A small variation was observed in the  $FF$  values for liquid electrolyte/conventional PVdF-*co*-HF-based polymer electrolyte (0.63) and ML-0249-embedded PVdF-*co*-HFP-based polymer electrolyte (0.65). The E7-embedded PVdF-*co*-HFP-based polymer electrolyte has an even higher  $V_{oc}$  (0.71 V), which approaches that of the liquid electrolyte (0.72 V). Importantly,  $V_{oc}$  is 0.05 V larger for the E7-embedded PVdF-*co*-HFP-based polymer electrolyte than the conventional PVdF-*co*-HFP-based electrolyte.

The remarkably high efficiency enhancements observed for DSSCs in which LCs are added to the conventional PVdF-

**Table I.** Photovoltaic Performances Including Ionic Conductivity Data of DSSCs Comprised of a Liquid Electrolyte, PVdF-*co*-HFP Polymer Electrolytes, and LC-Emedded PVdF-*co*-HFP Polymer Electrolytes

Electrolyte	$J_{sc}$ (mA/cm <sup>2</sup> )	$V_{oc}$ (V)	$FF$ (%)	PCE (%)	Ionic Conductivity <sup>a</sup> (S/cm)
PVdF- <i>co</i> -HFP	14.53	0.66	63	6.07	$1.90 \times 10^{-2}$
ML-0249:PVdF- <i>co</i> -HFP	14.60	0.68	65	6.42	$2.33 \times 10^{-2}$
E7:PVdF- <i>co</i> -HFP	14.03	0.71	64	6.34	$1.85 \times 10^{-2}$
Liquid Electrolyte	15.29	0.72	63	7.17	$3.63 \times 10^{-2}$

<sup>a</sup>Ionic conductivity was measured at the temperature of 25 °C.

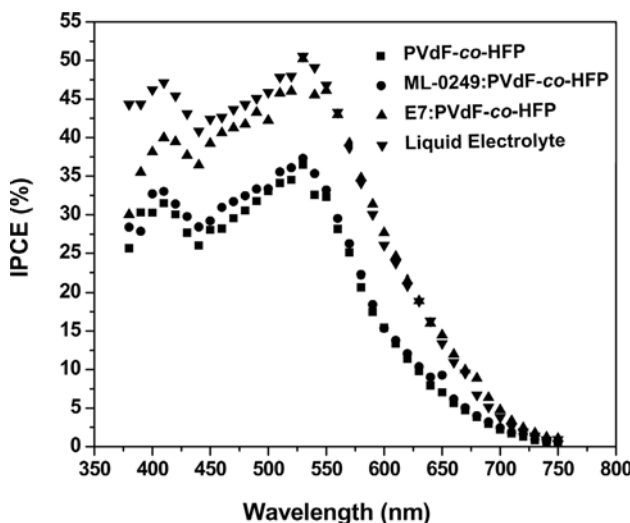


Figure 6. IPCE spectra for DSSCs.

*co*-HFP-based polymer electrolyte are a result of increases in both the number of pathways for electron injection and the rate of dye regeneration. These findings suggest that the promotion of exchange reactions by the two-dimensional electron conductive pathways in each domain could lead to improvements of  $J_{sc}$ .<sup>31</sup> Upon addition of LCs to the electrolyte, the PCEs of the DSSCs rise from 6.07 to 6.42%, a change of 0.35%. It is clear that LCs have a beneficial effect on dye adsorbed nanocrystalline TiO<sub>2</sub> used in the DSSCs. This is a consequence of structural differences between conventional PVdF-*co*-HFP-based polymer electrolytes and those containing embedded LCs.<sup>32</sup>

The IPCE data for DSSCs, fabricated using the PVdF-*co*-HFP-based polymer electrolyte, LC-embedded PVdF-*co*-HFP-based electrolytes and a liquid electrolyte are given in Figure 6. The data clearly show that the IPCE for the DSSC formed from the conventional PVdF-*co*-HFP-based polymer electrolyte contains two maxima at 409 and 529 nm, as has been described previously.<sup>24</sup> The E7-embedded PVdF-*co*-HFP-based polymer electrolyte containing DSSC reaches a maximum IPCE of *ca.* 50%, which is similar to the value associated with that of the DSSC comprised of a liquid electrolyte (51% at 520 nm). This observation appears to be a result of efficient penetration of the E7-embedded PVdF-*co*-HFP-based polymer electrolyte throughout the dye-sensitized TiO<sub>2</sub> surface, and formation of a two dimensional layered structure between the electrodes that reduce the restriction of the redox couple contact.

## Conclusions

Novel DSSCs containing LC-embedded, PVdF-*co*-HFP-based, polymer electrolytes were fabricated in the study described above. The DSSC, formed using the conventional PVdF-*co*-HFP-based polymer electrolyte, gives rise to a

PCE value of 6.07% at one sun light. The photovoltaic performances of DSSCs were observed to increase when LCs are incorporated in the PVdF-*co*-HFP-based polymer electrolyte. For example, the ML-0249-embedded PVdF-*co*-HFP-based polymer electrolyte has  $V_{oc}$  (0.68 V) and  $J_{sc}$  (14.60 mA/cm<sup>2</sup>) values that are greater than those formed using the conventional PVdF-*co*-HFP-based polymer electrolyte  $V_{oc}$  (0.66 V) and  $J_{sc}$  (14.53 mA/cm<sup>2</sup>).

It appears that LC-embedded PVdF-*co*-HFP-based polymer electrolytes have greater interfacial contacts between the N719 dye adsorbed photoanode and the counter electrode. This would play a crucial role in increasing the PCE of DSSCs generated from conventional *versus* LC polymer electrolytes from 6.07 to 6.42% and the respective ionic conductivity from  $1.9 \times 10^{-2}$  to  $2.33 \times 10^{-2}$  S/cm. The DSSC containing the E7-embedded PVdF-*co*-HFP-based polymer electrolyte has a maximum IPCE value of 50%, which is near to that of a liquid electrolyte containing DSSC (51%). Overall, the results of this investigation show that the new LC based polymer electrolyte strategy can be used to construct DSSCs that have enhanced photovoltaic performances and long term thermal stabilities. Further studies of this strategy are in progress.

**Acknowledgement.** This work was supported by the Korea Science and Engineering Foundation (KOSEF) grant funded by the Korea government (MEST) (No. M10600000157-06J0000-15710, R11-2008-088-01-003-0). This study was financially supported by Pusan National University inprogram, Post-Doc. 2008.

## References

- (1) B. O'Regan and M. Grätzel, *Nature*, **353**, 737 (1991).
- (2) M. Grätzel, *Nature*, **414**, 338 (2001).
- (3) R. D. McConnell, *Renewable Sustainable Energy Rev.*, **6**, 273 (2002).
- (4) M. K. Nazeeruddin, F. D. Angelis, S. Fantacci, A. Selloni, G. Viscardi, P. Liska, S. Ito, B. Takeru, and M. Grätzel, *J. Am. Chem. Soc.*, **127**, 16835 (2005).
- (5) W. Kubo, T. Kitamura, K. Hanabusa, Y. Wada, and S. Yanagida, *Chem. Comm.*, 374 (2002).
- (6) H. X. Wang, H. Li, B. F. Xue, Z. X. Wang, Q. B. Meng, and L. Q. Chen, *J. Am. Chem. Soc.*, **127**, 6394 (2005).
- (7) S. Murali, S. Mikoshiba, H. Sumino, T. Kato, and S. Hayase, *Chem. Comm.*, 1534 (2003).
- (8) B. O'Regan and D. T. Schwartz, *Chem. Mater.*, **10**, 1501 (1998).
- (9) B. O'Regan, F. Lenzmann, R. Muis, and J. Wienke, *Chem. Mater.*, **14**, 5023 (2002).
- (10) U. Bach, D. Lupo, P. Comte, and M. Grätzel, *Nature*, **395**, 583 (1998).
- (11) R. Senadeera, N. Fukuri, and Y. Satio, *Chem. Comm.*, 2259 (2005).
- (12) M. Grätzel, *Prog. Photovoltaics*, **8**, 171 (2000).
- (13) A. F. Nogueira, C. Longo, and M. A. De Paoli, *Coord. Chem. Rev.*, **248**, 1455 (2004).

- (14) H. Lee, W. Kim, S. Park, W. Shin, S. Jin, J. Lee, S. Han, K. Jung, and M. Kim, *Macromol. Symp.*, **235**, 230 (2006).
- (15) M. R. Kim, W. S. Shin, W. S. Kim, H. J. Lee, S. H. Park, J. K. Lee, and S. H. Jin, *Mol. Cryst. Liq. Cryst.*, **462**, 91 (2007).
- (16) W. S. Shin, S. C. Kim, S. J. Lee, H. S. Jeon, M. K. Kim, B. Vijaya Kumar Naidu, S. H. Jin, J. K. Lee, J. W. Lee, and Y. S. Gal, *J. Polym. Sci. Part A: Polym. Chem.*, **45**, 1394 (2007).
- (17) M. A. Karim, Y. R. Cho, J. S. Park, S. C. Kim, H. J. Kim, J. W. Lee, Y. S. Gal, and S. H. Jin, *Chem. Comm.*, 1929 (2008).
- (18) F. Cao, G. Oskam, and P. C. Searson, *J. Phys. Chem. B*, **99**, 17071 (1995).
- (19) O. A. Ileperuma, M. A. K. L. Dissanayake, and S. Somasundaram, *Electrochim. Acta*, **47**, 2801 (2002).
- (20) M. G. Kang, K. M. Kim, K. S. Ryu, S. H. Chang, N. G. Park, J. S. Hong, and K. J. Kim, *J. Electrochem. Soc.*, **151**, E257 (2004).
- (21) J. Wu, Z. Lan, J. Lin, M. Huang, S. Hao, T. Sato, and S. Yin, *Adv. Funct. Mater.*, **19**, 4006 (2007).
- (22) T. Kato, A. Okazaki, and S. Hayase, *Chem. Comm.*, 363 (2005).
- (23) V. Suryanarayanan, K. M. Lee, W. H. Ho, H. C. Chen, and K. C. Ho, *Sol. Energy Mater. Sol. Cells*, **91**, 1467 (2007).
- (24) P. Wang, S. M. Zakeeruddin, I. Exnar, and M. Grätzel, *Chem. Comm.*, 2972 (2002).
- (25) P. S. Wang, S. M. Zakeeruddin, and M. Grätzel, *J. Fluorine Chem.*, **125**, 1241 (2004).
- (26) P. Wang, S. M. Zakeeruddin, J. E. Moser, M. K. Nazeeruddin, T. Sekiguchi, and M. Grätzel, *Nat. Mater.*, **2**, 402 (2003).
- (27) J. S. Wilkes and M. J. Zaworotko, *J. Chem. Soc. Chem. Comm.*, 965 (1992).
- (28) T. Welton, *Chem. Rev.*, **99**, 2071 (1999).
- (29) M. A. B. H. Susan, T. Kaneko, A. Noda, and M. Watanabe, *J. Am. Chem. Soc.*, **127**, 4976 (2005).
- (30) P. Wang, Q. Dai, S. M. Zakeeruddin, M. Forsyth, D. R. MacFarlane, and M. Grätzel, *J. Am. Chem. Soc.*, **126**, 13590 (2004).
- (31) N. Yamanaka, R. Kawano, W. Kubo, T. Kitamura, Y. Wada, M. Watanabe, and S. Yanagida, *Chem. Comm.*, 740 (2005).
- (32) R. Kawano, M. K. Nazeeruddin, A. Sato, M. Grätzel, and M. Watanabe, *Electrochim. Commun.*, **9**, 1134 (2007).